

# PULSE-FRONT TILT CAUSED BY THE USE OF A GRATING MONOCHROMATOR AND SELF-SEEDING OF SOFT X-RAY FELS

G. Geloni, European XFEL GmbH, Hamburg, Germany  
 V. Kocharyan and E. Saldin, DESY, Hamburg, Germany

## Abstract

Self-seeding is a promising approach to significantly narrow the SASE bandwidth of XFELs to produce nearly transform-limited pulses. The development of such schemes in the soft X-ray wavelength range necessarily involves gratings as dispersive elements. These introduce, in general, a pulse-front tilt, which is directly proportional to the angular dispersion. Pulse-front tilt may easily lead to a seed signal decrease by a factor two or more. Suggestions on how to minimize the pulse-front tilt effect in the self-seeding setup are given. More details and references can be found in [1].

## INTRODUCTION

The longitudinal coherence of X-ray SASE FELs is rather poor. Self-seeding schemes have been studied to reduce the bandwidth of SASE X-ray FELs. A self-seeding setup consists of two undulators separated by a photon monochromator and an electron bypass, normally a four-dipole chicane. Recently, a very compact soft X-ray self-seeding scheme was designed at SLAC, based on a grating monochromator. We studied the performance of this compact scheme for the European XFEL upgrade elsewhere (see [1] for references). Limitations on the performance of the self-seeding scheme related with aberrations and spatial quality of the seed beam have been extensively discussed in literature and go beyond the scope of this paper. Here we will focus our attention on the spatiotemporal distortions of the X-ray seed pulse. Numerical results provided by ray-tracing algorithms applied to grating design programs give accurate information on the spatial properties of the imaging optical system of grating monochromator. However, in the case of self-seeding, the spatiotemporal deformation of the seeded X-ray optical pulses is not negligible: aside from the conventional aberrations, distortions as pulse-front tilt should also be considered (see [1] for references). The propagation and distortion of X-ray pulses in grating monochromators can be described using a wave optical theory. Most of our calculations are, in principle, straightforward applications of conventional ultrafast pulse optics. Our paper provides physical understanding of the self-seeding setup with a grating monochromator, and we expect that this study can be useful in the design stage of self-seeding setups.

## THEORETICAL BACKGROUND

### Pulse-front Tilt from Gratings

Ultrashort X-ray FEL pulses are usually represented as products of electric field factors separately dependent on

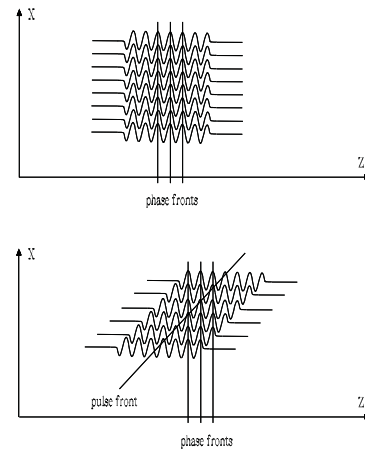


Figure 1: An undistorted pulse beam (left) and a beam with pulse front tilt (right) (adapted from literature, see [1] for references).

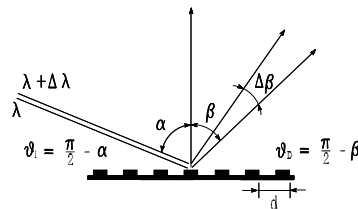


Figure 2: Geometry of diffraction grating scattering.

space and time. The assumption of separability of the spatial (or spatial frequency) dependence of the pulse from the temporal (or temporal frequency) dependence is usually made for the sake of simplicity. However, when the manipulation of ultrashort X-ray pulses requires the introduction of coupling between spatial and temporal frequency coordinates, such assumption fails. The direction of energy flow -usually identified as rays directions- is always orthogonal to the surface of constant phase, that is to the wavefronts of the corresponding propagating wave. If one deals with ultrashort X-ray pulses, one has to consider, in addition, planes of constant intensity, that is pulse fronts. Fig. 1 shows a schematic representation of the electric field profile of an undistorted pulse and one with a pulse-front tilt. A distortion of the pulse front does not affect propagation, because the phase fronts remain unaffected. However, for most applications, including self-seeding applications, it is desirable that these fronts be parallel to the phase fronts, and therefore orthogonal to the propagating

direction. A pulse-front tilt can be present in the beam due to the propagation through a grating monochromator. As shown in Fig. 2, the input beam is incident on the grating at an angle  $\theta_i$ . The diffracted angle  $\theta_D$  is a function of frequency, according to the well-known plane grating equation. Assuming diffraction into the first order, one has  $\lambda = d(\cos \theta_i - \cos \theta_D)$ , where  $\lambda = 2\pi c/\omega$ , and  $d$  is the groove spacing. This describes the basic working of a grating monochromator. By differentiating this equation one obtains  $\frac{d\theta_D}{d\lambda} = \frac{1}{\theta_D d}$ , where we assume grazing incidence geometry,  $\theta_i \ll 1$  and  $\theta_D \ll 1$ . The physical meaning is that different spectral components of the outgoing pulse travel in different directions. The electric field of a pulse including angular dispersion can be expressed in the Fourier domain  $\{k_x, \omega\}$  as  $E(k_x - p\omega, \omega)$ , while the inverse Fourier transform from the  $\{k_x, \omega\}$  domain to the space-time domain  $\{x, t\}$  can be expressed as  $E(x, t + px)$ , which is the electric field of a pulse with a pulse-front tilt. The tilt angle  $\gamma$  is given by  $\tan \gamma = cp$ . More specifically  $p = \frac{dk_x}{d\omega} = k \frac{d\theta_D}{d\omega} = \frac{\lambda}{c} \frac{d\theta_D}{d\lambda} = \frac{\lambda}{c\theta_D d}$ . Therefore one concludes that the pulse-front tilt is invariably accompanied by angular dispersion. It follows that any device like a grating monochromator, that introduces an angular dispersion, also introduces significant pulse-front tilt, which is problematic for seeding.

### Transformation of FEL Pulses by Crystals

The development of self-seeding schemes in the hard X-ray wavelength range necessarily involves crystal monochromators. Recently, the spatiotemporal coupling in the electric field relevant to self-seeding schemes with crystal monochromators has been analyzed in the frame of classical dynamical theory of X-ray diffraction by Lindberg and Shvyd'ko (see [1] for references). This analysis shows that a crystal in Bragg reflection geometry transforms the incident electric field  $E(x, t)$  in the  $\{x, t\}$  domain into  $E(x - at, t)$ , that is the field of a pulse with a less well-known distortion. The physical meaning of this distortion is that the beam spot size is independent of time, but the beam central position changes as the pulse evolves in time. One of the aims of this subsection is to disentangle what is specific to the transformation by a crystal and what is intrinsic to the grating case. Our purpose here is not that of presenting novel results but, rather, to attempt a more intuitive explanation of spatiotemporal coupling phenomena in the dynamical theory of X-ray diffraction, and to convey the importance and simplicity of already known results. We begin our analysis by specifying the scattering geometry under study. The angle between the physical surface of the crystal and the reflecting atomic planes is an important factor. The reflection is said to be symmetric if the surface normal is perpendicular to the reflecting planes in the case of Bragg geometry. We shall examine only the symmetric Bragg case. Let us consider an electromagnetic plane wave in the X-ray frequency range incident on an infinite, perfect crystal. Within the kinematical approximation, according to the Bragg law, constructive in-

terference of waves scattered from the crystal occurs if the angle of incidence,  $\theta_i$  and the wavelength,  $\lambda$ , are related by the well-known relation  $\lambda = 2d \sin \theta_i$ , assuming reflection into the first order. This equation shows that for a given wavelength of the X-ray beam, diffraction is possible only at certain angles determined by the interplanar spacings  $d$ . It is important to remember the following geometrical relationships:

1. The angle between the incident X-ray beam and normal to the reflection plane is equal to that between the normal and the diffracted X-ray beam. In other words, Bragg reflection is a mirror reflection, and the incident angle is equal to the diffracted angle ( $\theta_i = \theta_D$ ).
2. The angle between the diffracted X-ray beam and the transmitted one is always  $2\theta_i$ . In other words, incident beam and forward diffracted (i.e. transmitted) beam have the same direction.

We now turn our attention beyond the kinematical approximation to the dynamical theory of X-ray diffraction by a crystal. An optical element inserted into the X-ray beam is supposed to modify some properties of the beam as its width, its divergence, or its spectral bandwidth. It is useful to describe the modification of the beam by means of a transfer function. The reflectivity curve - the reflectance - in Bragg geometry can be expressed in the frame of dynamical theory as  $R(\theta_i, \omega) = R(\Delta\omega + \omega_B \Delta\theta \cot \theta_B)$ , where  $\Delta\omega = (\omega - \omega_B)$  and  $\Delta\theta = (\theta_i - \theta_B)$  are the deviations of frequency and incident angle of the incoming beam from the Bragg frequency and Bragg angle, respectively. The frequency  $\omega_B$  and the angle  $\theta_B$  are given by the Bragg law:  $\omega_B \sin \theta_B = \pi c/d$ . We follow the usual procedure of expanding  $\omega$  in a Taylor series about  $\omega_B$ . Consider a perfectly collimated, white beam incident on the crystal. In kinematical approximation  $R$  is a Dirac  $\delta$ -function, which is simply represented by the differential form of Bragg law:  $d\lambda/d\theta_i = \lambda \cot \theta_i$ . In contrast to this, in dynamical theory the reflectivity width is finite. This means that there is a reflected beam even when incident angle and wavelength of the incoming beam are not related exactly by Bragg equation. It is interesting to note that the geometrical relationships 1. and 2. are still valid in the framework of dynamical theory. In particular, reflection in dynamical theory is always a mirror reflection. We underline here that if we have a perfectly collimated, white incident beam, we also have a perfectly collimated reflected beam. Its bandwidth is related with the width of the reflectivity curve. We will regard the beam as perfectly collimated when the angular spread of the beam is much smaller than the angular width of the transfer function  $R$ . It should be realized that the crystal does not introduce an angular dispersion similar to a grating or a prism. However, a more detailed analysis based on the expression for the reflectivity shows that a less well-known spatiotemporal coupling exists. The fact that the reflectivity is invariant under angle and frequency transformations obeying  $\Delta\omega + \omega_B \Delta\theta \cot \theta_B = \text{const}$  is evident, and corresponds to the coupling in the Fourier domain  $\{k_x, \omega\}$ . One might be surprised that the field trans-

formation for an XFEL pulse after a crystal in the  $\{x, t\}$  domain is given by  $E_{\text{out}}(x, t) = E(x - ct \cot \theta_B, t)$ , where  $k_x = \omega_B \Delta \theta / c$ . In general, one would indeed expect the transformation to be symmetric in both the  $\{k_x, \omega\}$  and in the  $\{x, t\}$  domain due to the symmetry of the transfer function. However, it is reasonable to expect the influence of a nonsymmetric input beam distribution. In the self-seeding case, the incoming XFEL beam is well collimated, meaning that its angular spread is a few times smaller than angular width of the transfer function. Only the bandwidth of the incoming beam is much wider than the bandwidth of the transfer function. In this limit, we can approximate the transfer function in the expression for the inverse temporal Fourier transform as a Dirac  $\delta$ -function. This gives  $E_{\text{out}}(x, t) = \xi(t)b(x - ct \cot \theta_B)$ , where  $\xi(W)$  is the inverse Fourier transform of the reflectivity curve. In the opposite limit when the incoming beam has a wide angular width and a narrow bandwidth we take the transfer function in the inverse spatial Fourier transform as a Dirac  $\delta$ -function. This gives  $E_{\text{out}}(x, t) = \xi(x \tan \theta_B / c)a(t - (x/c) \tan \theta_B)$ . These two limits represent the two sides of the symmetry of the transfer function. The last expression  $E_{\text{out}}(x, t)$  is the field of a pulse with a pulse front tilt. Typically one would think that a pulse front tilt can be introduced only by dispersive elements like gratings or prisms. Here we presented an example in which no dispersive elements exists, and we stress that angular dispersion can be introduced by non dispersive element like crystals too. Although we began by considering a case of reflection transfer function in Bragg reflection geometry, none of our arguments depends on that fact. The relation for the reflectance still holds if the transfer function  $R$  is referred to the transmittance in Bragg reflection geometry. For the transmitted beam, all derivations are worked out in the same way we have done here and gives asymptotic expression for field of forward scattered pulses.

### MODELING OF SELF-SEEDING SETUP

A self-seeding setup should be compact enough to fit one undulator segment. In this case its installation does not perturb the undulator focusing system and allows for the safe return to the baseline mode of operation. The design adopted for the LCLS is the novel one by Y. Feng et al. (see [1] for references), and is based on a planar VLS grating. It is equipped only with an exit slit. Such design includes four optical elements, a cylindrical and spherical focusing mirrors, a VLS grating and a plane mirror in front of the grating. The optical layout of the monochromator is schematically shown in Fig. 3.

A simplified diagram for analyzing the grating monochromator is shown in Fig. 4. We will assume that the optical system used for imaging purposes is the well-known two-lens image formation system. With reference to Fig. 3, the VLS grating is represented by a combination of a planar grating with fixed line spacing and a lens, with the focal length of the lens equal to the focal length of the VLS grating. The analysis of the grating monochromator

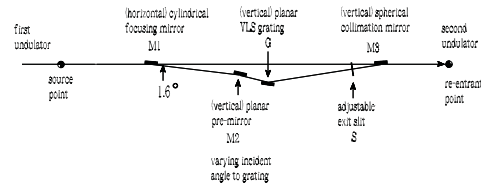


Figure 3: Optics for the compact grating monochromator originally proposed at SLAC (see [1] for references) for the soft X-ray self-seeding setup.

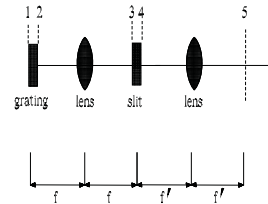


Figure 4: Diagram of the self-seeding grating monochromator used in theoretical analysis (adapted from literature, see [1] for references).

is simplified by recognizing that the grating can be shifted from a position immediately before the lens to a position immediately after the object plane. The monochromator is treated assuming no aberrations. This approximation is useful, since for the design shown on Fig. 3 the aberration effects are negligible (see [1] for references). This simplifies calculations and allows analytical results to be derived. The angular dispersion of the grating causes a separation of different optical frequencies at the Fourier plane of the first focusing element (lens). Therefore, this system becomes a tunable frequency filter if a slit is placed at the Fourier plane. We assume that the two lenses in Fig. 4 are not identical, so that this scheme allows for magnification by changing the focal distance of the second lens. It is important to analyze the output field from the grating monochromator quantitatively. In [1] we calculated analytically the propagation of the input signal to different planes of interest within the self-seeding monochromator, as indicated in Fig. 4. Here we will simply present some of the conclusions in [1].

We fix the slit function  $S$  as  $S(x) = 1$  for  $|x| < d_s$  and  $S(x) = 0$  for  $|x| > d_s$ . Given a slit with half size  $d_s$ , we introduce a normalized notion of slit size  $\alpha = \frac{d_s}{\sigma_f} = d_s \frac{k\sigma}{\beta f}$ . It is possible to show the output characteristics of the radiation as a function of the slit size by means of universal plots. We first consider the resolving power  $R = (\Delta\omega/\omega)_{\text{FWHM}}^{-1}$ . We introduce the resolving power  $R_n$  normalized to the inverse of the maximal bandwidth, that is the bandwidth in the limiting case for  $\alpha \ll 1$ , as  $R_n = R \left( \frac{1.18\theta_s d}{2\pi\sigma} \right)$ . The behavior of  $R_n$  as a function of  $\alpha$  is shown in Fig. 5. The resolution of monochroma-

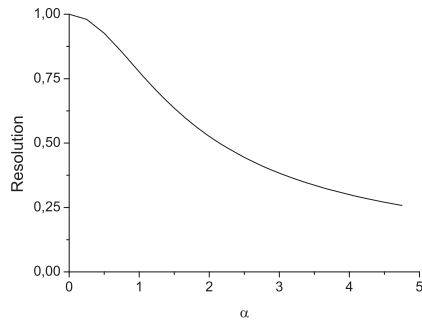


Figure 5: Resolving power normalized to the asymptotic case for  $\alpha \ll 1$  as a function of  $\alpha$ .

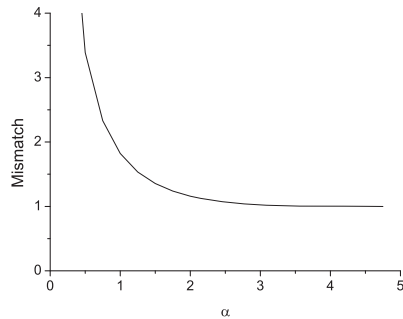


Figure 6: Transverse spot size of the photon beam normalized to the asymptotic case for  $\alpha \gg 1$  as a function of  $\alpha$ . We assume  $f\theta_i/f'\theta_D = 1$ .

tor increases as the slit size decreases. The 90% of the maximal resolution level is met for normalized slit width less than  $\alpha < 1$ . However, the energy of the seed pulse decreases proportionally to the decrease of the slit width. Moreover, decreasing the slit width will also cause an increase of the output beam size. This will lead to spatial mismatch between the seed beam and the FEL mode in the second undulator. The relationship between the beam

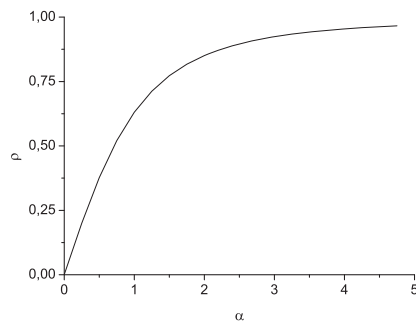


Figure 7: Dependence of the spatiotemporal coupling as a function of  $\alpha$ .

transverse size (in terms of FWHM) and slit width is shown in Fig. 6, where we plot the transverse spot size of the photon beam normalized to the asymptotic case for  $\alpha \gg 1$  as a function of  $\alpha$ . To summarize, it is not recommended that the normalized slit width be narrower than unity if a reasonable seed field amplitude is required. Finally, a useful figure of merit measuring the spatiotemporal coupling can be found in literature (see [1] for references). Considering the angular dispersion this parameter can be written as  $\rho = \int dk_x d\Delta\omega I \cdot \frac{k_x \Delta\omega}{\langle (\delta k_x)^2 \rangle^{1/2} \langle (\delta\omega)^2 \rangle^{1/2}}$ , where  $\langle (\delta k_x)^2 \rangle = \int dk_x d\Delta\omega I(k_x, \Delta\omega) k_x^2$ ,  $\langle (\delta\omega)^2 \rangle = \int dk_x d\Delta\omega I(k_x, \Delta\omega) \Delta\omega^2$ ,  $I(k_x, \Delta\omega) = |E(k_x, \Delta\omega)|^2$ . The range of  $\rho$  is in  $[-1, 1]$  and readily indicate the severity of these distortions. To estimate the pulse front tilt distortion calculate the pulse front tilt parameter  $\rho$  as a function of the slit width  $\alpha$ . The results are shown in Fig. 7. It is found to be larger than 50% for a slit width  $\alpha > 1$ . Therefore, standard tuning of the seed monochromator will lead to significant spatiotemporal coupling in the seed pulses. The effect of pulse front tilt distortion can be reduced if the slit width will be narrower than  $\alpha < 1$ . However, the reduction of the pulse front tilt influence is accompanied by significant loss in seed signal amplitude. On the one hand, decreasing the slit width increases the resolving power and suppresses the pulse front tilt distortion. On the other hand, it decreases the seed power and increases the transverse mismatch with the FEL mode in the second undulator. As a result, a tradeoff must be reached between achievable resolution and effective level of the input signal. Transverse coherence of XFEL radiation is settled without seeding. This is due to the transverse eigenmode selection mechanism: roughly speaking, only the ground eigenmode survives at the end of amplification process. It follows that the spatiotemporal distortions of the seed pulse do not affect the quality of the output radiation. They only affect the input signal value. Therefore, the relevant value for self-seeded operation is the input coupling factor between the seed pulsed beam and the ground eigenmode of the FEL amplifier. In order to model the performance of a soft X-ray self-seeded FEL with a grating monochromator, one naturally starts with the grating monochromator optical system. One aspect of optimizing the output characteristics of the self-seeded FEL involves the specification of spectral width, peak power, pulse-front tilt parameter and transverse size of the seed pulse as a function of the slit width. This can be achieved by purely analytical methods. Another aspect of the problem is the modeling of the FEL process including a seed pulse with spatio-temporal distortions and transverse mismatching with the ground FEL eigenmode. This study can be made only with numerical simulation code, and is left for the future.

## REFERENCES

- [1] G. Geloni, V. Kocharyan and E. Saldin, "Pulse-front tilt caused by the use of a grating monochromator and self-seeding of soft X-ray FELs", DESY 12-051, <http://arxiv.org/abs/1203.6442> (2012).